

ACCRETION-POWERED STELLAR WINDS III: SPIN EQUILIBRIUM SOLUTIONS

SEAN MATT¹ AND RALPH E. PUDRITZ²

¹Department of Astronomy, University of Virginia, P.O. Box 400325, Charlottesville, VA 22904-4325; seanmatt@virginia.edu and
²Physics and Astronomy Department, McMaster University, Hamilton, ON L8S 4M1, Canada; pudritz@physics.mcmaster.ca

Draft version June 15, 2021

ABSTRACT

We compare the stellar wind torque calculated in a previous work (Paper II) to the spin-up and spin-down torques expected to arise from the magnetic interaction between a slowly rotating ($\sim 10\%$ of breakup) pre-main-sequence star and its accretion disk. This analysis demonstrates that stellar winds can carry off orders of magnitude more angular momentum than can be transferred to the disk, provided that the mass outflow rates are greater than the solar wind. Thus, the equilibrium spin state is simply characterized by a balance between the angular momentum deposited by accretion and that extracted by a stellar wind. We derive a semi-analytic formula for predicting the equilibrium spin rate as a function only of the ratio of \dot{M}_w/\dot{M}_a and a dimensionless magnetization parameter, $\Psi \equiv B_*^2 R_*^2 (\dot{M}_a v_{\text{esc}})^{-1}$, where \dot{M}_w is the stellar wind mass outflow rate, \dot{M}_a the accretion rate, B_* the stellar surface magnetic field strength, R_* the stellar radius, and v_{esc} the surface escape speed. For parameters typical of accreting pre-main-sequence stars, this explains spin rates of $\sim 10\%$ of breakup speed for $\dot{M}_w/\dot{M}_a \sim 0.1$. Finally, the assumption that the stellar wind is driven by a fraction of the accretion power leads to an upper limit to the mass flow ratio of $\dot{M}_w/\dot{M}_a \lesssim 0.6$.

Subject headings: accretion, accretion disks — MHD — stars: magnetic fields — stars: pre-main-sequence — stars: rotation — stars: winds, outflows

1. INTRODUCTION

The slow rotation rates of low to intermediate mass ($\lesssim 2M_\odot$) pre-main-sequence stars remains one of the most important aspects of star formation that has, so far, resisted a generally accepted explanation. By the time they become optically visible as T Tauri stars (TTSS; Joy 1945), approximately half of them are observed to rotate at approximately 10% of breakup speed (the “slow rotators”; e.g., Vogel & Kuhi 1981; Bouvier et al. 1997; Rebull et al. 2004; Herbst et al. 2007). This is a surprise because many TTSSs (the Classical T Tauri stars; CTTSSs) are actively accreting material from surrounding Keplerian disks (Lynden-Bell & Pringle 1974; Bertout et al. 1988; Calvet & Gullbring 1998; Muzerolle et al. 2001). At a typical accretion rate of $\dot{M}_a \sim 10^{-8} M_\odot \text{ yr}^{-1}$, the angular momentum deposited by accreting disk material should spin up a CTTS to near breakup speed in $\sim 10^6$ years (Hartmann & Stauffer 1989; Matt & Pudritz 2007). Since the accretion phase lasts for $10^6 - 10^7$ years (Lyo & Lawson 2005; Jayawardhana et al. 2006), since the stars accrete at much higher rates prior to the TTS phase, and since the stars are still contracting (Rebull et al. 2002), an efficient angular momentum loss mechanism is required to explain the existence of the slow rotators.

A few interesting and important ideas for explaining the TTS slow rotators have been developed over the last two decades. These have resulted in the star-disk interaction model of Ghosh & Lamb (1978), applied to CTTSSs by Königl (1991, and see Camenzind 1990), the X-wind model (Shu et al. 1994), and the idea that stellar winds provide strong torques (Hartmann & Stauffer 1989; Tout & Pringle 1992; Paatz & Camenzind 1996; Ferreira et al. 2000; Matt & Pudritz 2005a). Although

both have advanced our understanding of the magnetic star-disk interaction, neither the Ghosh & Lamb nor X-wind models are without problems (Ferreira et al. 2000; Uzdensky 2004; Matt & Pudritz 2005b), and the idea that stellar winds are important has not yet been worked out in sufficient detail to compare to the other models.

In Matt & Pudritz (2005a, hereafter Paper I), we further explored powerful stellar winds as a solution to the angular momentum problem and suggested that a fraction of the accretion power provides the energy necessary to drive the wind. We showed that stellar winds are capable of carrying off the accreted angular momentum, provided that $\dot{M}_w/\dot{M}_a \sim 0.1$, where \dot{M}_w is the outflow rate of material that is magnetically connected to the star (the “stellar wind”). This analysis included a formulation for the stellar wind torque that contained the Alfvén radius (r_A), which is not easily determined a priori in the wind, and the conclusions were based on a one-dimensional scaling estimate of this important physical quantity. Thus, while it is clear that accretion-powered stellar winds (APSWs) can in principle provide the necessary spin-down torque, this idea requires further development to produce a more detailed model.

Toward this goal, Matt & Pudritz (2008, hereafter Paper II) used 2-dimensional (axisymmetric) magnetohydrodynamic simulations to solve for r_A and calculate realistic stellar wind torques for a range of parameters. In the present paper, we use the stellar wind solutions of Paper II to compare the stellar wind torque to the torques expected to arise from the star-disk interaction. Furthermore, we find new solutions for stellar spins, based upon torque balance between the accretion torque and the APSW spin-down torque. This paper begins with a brief description of the simulation results of Paper II (§2). We then compare the stellar wind torque to the

TABLE 1
FIDUCIAL STELLAR WIND
PARAMETERS

Parameter	Value
M_*	$0.5 M_\odot$
R_*	$2.0 R_\odot$
B_* (dipole)	200 G
f	0.1
\dot{M}_w	$1.9 \times 10^{-9} M_\odot \text{ yr}^{-1}$
c_s/v_{esc}	0.222
γ	1.05

star-disk spin-down torque in section 3 and then to the star-disk spin-up torque in section 4, which contains spin-equilibrium solutions. Section 5 contains a summary and discussion.

2. RESULTS OF STELLAR WIND SIMULATIONS

This section contains a brief description of the simulation results of Paper II that we will use for our analysis, and the reader will find details in that paper. The primary purpose of the simulations was to compute the spin-down torque on a star, due to the angular momentum outflow in a wind. We used numerical magnetohydrodynamic simulations to directly calculate the torque τ_w from steady-state, 2D (axisymmetric) winds from isolated stars. We adopted coronal (thermal-pressure-driven) winds as a proxy for the unknown wind driving mechanism. In the simulations, the torque is entirely determined by the seven key parameters listed in table 1. These are the stellar mass, M_* ; stellar radius, R_* ; strength of the rotation-axis-aligned dipole magnetic field at the surface and equator of the star, B_* ; spin rate expressed as a fraction of breakup speed,

$$f \equiv \Omega_* R_*^{3/2} (GM_*)^{-1/2}, \quad (1)$$

where Ω_* is the angular spin rate of the star; mass outflow rate in the stellar wind, \dot{M}_w ; ratio of the thermal sound speed to the escape speed, evaluated at the base of the wind (just above the stellar surface), c_s/v_{esc} ; and adiabatic index, γ .

Table 1 lists the value of each parameter adopted for a fiducial case. Paper II contained a parameter study in which each of the seven parameters were varied relative to the fiducial case, and 14 cases from the parameter study are listed in table 2¹. In each case, six of the parameters were held fixed at the fiducial value (as given in table 1), and one parameter was varied as indicated by the first column of table 2.

To compare with analytic theory, we also calculated the effective Alfvén radius (r_A), where the poloidal wind velocity equals the poloidal Alfvén speed, using an analytic formula for the stellar wind torque,

$$\tau_w = -\dot{M}_w \Omega_* \langle r_A^2 \rangle. \quad (2)$$

Since our simulations are multi-dimensional, we have used $\langle r_A^2 \rangle$, which is the mass-loss-weighted average of r_A^2 . Hereafter, we'll refer to $\langle r_A^2 \rangle^{1/2}$ generically as r_A .

¹ In this paper, we do not discuss the cases from Paper II that include a quadrupole magnetic field, nor the extremely slow rotator case (with $f = 0.004$).

Using the simulation result for τ_w , equation 2 defines the value of r_A , which is tabulated for all cases in the second column of table 2.

In this paper, we make use of the semi-analytic formulation for the Alfvén radius from Paper II,

$$\frac{r_A}{R_*} = K \left(\frac{B_*^2 R_*^2}{\dot{M}_w v_{\text{esc}}} \right)^m, \quad (3)$$

where K and m are dimensionless constants fit to the simulation, and $v_{\text{esc}} = (2GM_*/R_*)^{1/2}$ is the escape speed from the stellar surface. Paper II showed that the values of $K \approx 2.11$ and $m \approx 0.223$ well-describe (to better than 1%) the fiducial case and those eight other cases with variations on B_* , R_* , \dot{M}_w , and M_* . Although this is only approximately valid for situations with different wind acceleration rates or different rotation rates (in which case the values of K and m are slightly different; see Paper II), the formulation of equation 3 serves well as an indication of the approximate dependence of the stellar wind on parameters, which will be important for discussing a wide range of possible conditions.

The form of equation (3) is similar to that derived by (e.g.) Pelletier & Pudritz (1992, and see Ferreira 1997) for the general theory of centrifugally driven disk winds. The quantity in brackets measures the magnetization of the wind. By assuming that the Alfvén speed $v_{r,A}$ (at the Alfvén radius) is directly proportional to $\Omega_* r_A$, a relation of the kind given by equation (3) can be derived (e.g., see equation 2.27 of Pelletier & Pudritz 1992). In that case, the value of the index is $m = 1/3$. While this value is not far from the results of our numerical simulations, the difference is significant. One key reason for this may be that disk winds are in the regime of so-called fast magnetic rotators, whereas the rather slowly rotating TTS are either slow magnetic rotators (where wind-driving forces dominate over centrifugal ones) or are intermediate between these two regimes (see Paper II).

For the discussion that follows, it is useful to highlight how the lever arm (r_A) and wind torque responds to changing the mass load (the mass loss rate) of the wind. The fact that the Alfvén lever arm in a hydromagnetic wind gets smaller as the mass load of the outflow increases, as is seen in equation (3), seems to suggest that the wind would become ineffective. This is certainly not true however, because equation (2) assures that an increase in wind mass loss rate leads to a net increase in the torque that the wind exerts upon the star (the net wind torque scales as \dot{M}_w^{1-2m}). This is the basic reason why, by having an outflow rate that is a substantial fraction of the accretion rate, an accretion-powered stellar wind can be effective in countering the accretion torque.

It is our goal here to compare the stellar wind torque to the torque expected to arise from the star-disk interaction, and the latter has only been determined thus far for a dipolar geometry. So we only consider here the cases from Paper II with a dipole magnetic field. We also adopt the following assumptions. Paper II indicated that the details of the wind driving have a relatively small, but not entirely negligible, effect on the stellar wind torque. In the absence of a detailed model for how APSWs are driven, we assume that the velocity profile of an APSW does not differ substantially from our simulations (Paper II), so that the calculated torques are valid. Secondly,

TABLE 2
STELLAR WIND ALFVÉN RADII AND COMPARISON
TO STAR-DISK SPIN-DOWN TORQUES

Case	r_A/R_*	τ_w/τ_{dsd} ($\beta = 0.1$)	τ_w/τ_{dsd} ($\beta = 0.01$)
fiducial	6.97	59	490
$f = 0.2$	6.26	23	200
$f = 0.05$	7.65	140	1200
$B_* = 400$ G	9.55	27	230
$B_* = 2$ kG	19.3	4.6	39
low \dot{M}_w^a	11.8	17	140
very low \dot{M}_w^a	16.7	6.7	57
$R_* = 1.5 R_\odot$	5.96	86	730
$R_* = 3 R_\odot$	8.75	34	280
$M_* = 0.25 M_\odot$	7.52	49	410
$M_* = 1 M_\odot$	6.42	70	590
$c_s/v_{\text{esc}} = 0.245$	6.64	53	440
$c_s/v_{\text{esc}} = 0.192$	7.23	63	530
$\gamma = 1.10$	7.79	72	610

^a The mass outflow rate in the low and very low \dot{M}_w cases is 1.9×10^{-10} and $3.8 \times 10^{-11} M_\odot \text{ yr}^{-1}$, respectively.

Paper II considered winds from isolated stars. Here, we will use the computed torques to develop the APSW scenario, in which stellar winds are accompanied by disk winds, accretion flows, and the general star-disk interaction (see figure 1 of Paper I). In reality, the accretion disk blocks a portion of the stellar wind, and it is not clear how much this will affect the stellar wind torque. For the present study, we will assume that the presence of the disk and accretion will not significantly influence the stellar wind torques as computed in Paper II.

3. STELLAR WIND VS. STAR-DISK SPIN-DOWN TORQUE

The magnetic interaction between the star and disk results in angular momentum transfer between the two. All models that calculate the torque on the star from this interaction are based on the framework constructed by Ghosh & Lamb (1978). In this general model, some of the stellar magnetic dipole flux connects to the accretion disk and conveys torques between the star and disk. The net torque can be separated into a spin-up part that adds angular momentum to the star and a spin-down part that removes angular momentum from the star, giving it back to the disk. In the absence of a stellar wind, a spin-down torque only arises when there is a magnetic connection between the star and the region of the disk outside the corotation radius,

$$R_{\text{co}} \equiv f^{-2/3} R_*. \quad (4)$$

It is assumed that the disk is capable of transporting away the excess angular momentum it receives from the star. The goal of this section is to compare the stellar wind torque to the spin-down torque arising from the star-disk magnetic connection, to determine under which circumstances each of these torques may be important and aid in the angular momentum loss from the star.

To calculate the star-disk spin-down torque, τ_{dsd} , we follow Matt & Pudritz (2005b, hereafter MP05b), who formulated a Ghosh & Lamb type model that includes the effect of the opening of magnetic field lines via the differential rotation between the star and disk. In this case, τ_{dsd} is calculated by considering only the magnetic

flux that remains closed (connected), parametrized as having an azimuthal twist of less than a critical angle, $\tan^{-1}(\gamma_c)$. Here we adopt the value of $\gamma_c = 1$ suggested by Uzdensky et al. (2002). By combining equation (9) and (22) of MP05b with equation (4), we find

$$\tau_{\text{dsd}} = -\frac{\chi(\beta)}{3} f^2 B_*^2 R_*^3, \quad (5)$$

where

$$\chi(\beta) \equiv \beta^{-1} [1 + (1 + \beta)^{-2} - 2(1 + \beta)^{-1}] \quad (6)$$

is a dimensionless function of the strength of the effective magnetic diffusion rate in the disk. This is parametrized by β , which for a standard α -disk (Shakura & Sunyaev 1973) is $\beta \equiv \alpha h (P_t r)^{-1}$, where α has its usual meaning, h is the disk scale height at radius r , and P_t is the turbulent magnetic Prandtl number². Small values of β correspond to strong coupling, and MP05b suggested that $\beta \sim 0.01$ was appropriate for real disks. For strong coupling (small β), the magnetic field will be highly twisted azimuthally, leading to more open flux and a weaker star-disk spin-down torque. For small β , $\chi(\beta) \approx \beta$, but $\chi(\beta)$ has a maximum value of 0.25 when $\beta = 1$ (e.g., see fig. 7 of MP05b).

Equation (5) indicates that the star-disk spin-down torque is completely independent of the accretion rate. This torque only requires that there exists a Keplerian disk outside R_{co} , to which the star can connect, and it does not matter whether or not there is net accretion onto the star. The dependence on the stellar spin rate f is due to the fact that when the star spins faster, R_{co} is closer to the star, where the magnetic field is stronger.

We compare the stellar wind torque computed in our simulations to the star-disk spin-down torque by listing the ratio τ_w/τ_{dsd} in the last two columns of table 2. We consider both a case with $\beta = 0.1$, resulting in $\chi \approx 0.0826$, and a case with $\beta = 0.01$, resulting in $\chi \approx 0.00980$. It is apparent that the simulated stellar wind torques are tens to hundreds of times greater than τ_{dsd} , the larger difference existing for smaller values of β .

Thus, for the simulated winds, we see empirically that the stellar wind is much more effective at spinning down the star than is the star-disk connection. This can be understood qualitatively as follows. In the stellar magnetosphere, any torque on the star is primarily conveyed by the azimuthal twisting of its magnetic field. In the case of the magnetic field connecting the star to the disk, there is a limit to how much the magnetic field can be twisted before the connection is lost (Uzdensky et al. 2002, MP05b). In the case of a stellar wind flowing along the field, there is no such limit on the twist. The larger the mass outflow rate in the wind, the less capable is the magnetic field to keep wind material corotating with the star, and so the larger will be the twist of the field.

To show the dominance of the stellar wind torque more generally and to identify the circumstances under which it might not dominate, we will use the semi-analytic formulation of equation (3). By combining equations (1) –

² Note that this β has no relation to the usual “plasma beta” parameter that often appears in MHD studies.

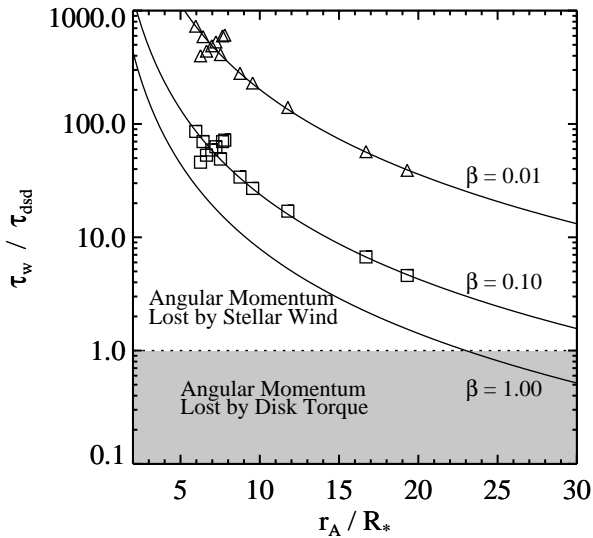


FIG. 1.— The ratio of the stellar wind torque to the spin-down portion of the star-disk interaction torque versus the magnetic lever arm length in the stellar wind. When the ratio is much greater than one, the stellar wind is most important for angular momentum loss from the star. The lines correspond to equation (8), assuming a stellar spin rate of $f = 0.1$ and three different values of the factor $\chi(\beta)$ (see text), corresponding to $\beta = 0.01, 0.1$, and 1 , as indicated. The values listed in table 2, obtained by comparing simulated wind torques to the analytic disk torques, are plotted as squares (for $\beta = 0.1$) and triangles ($\beta = 0.01$). The figure indicates that, unless the magnetic lever arm length is very long (e.g., for very low stellar wind mass loss rate), the spin-down torque from the disk is negligible.

(3), one obtains

$$\tau_w = -\frac{K^{1/m}}{\sqrt{2}} \left(\frac{R_*}{r_A}\right)^{1/m-2} f B_*^2 R_*^3 \quad (7)$$

for the stellar wind torque. At first it may seem unusual that τ_w is weaker when the magnetic lever arm length, r_A , is larger (for fixed $f B_*^2 R_*^3$). However this simply indicates that the stellar wind torque increases with increasing \dot{M}_w , as noted in section 2. Also, note that a weak f -dependence of r_A is not characterized in equation (3) (see Paper II), so the exact dependence of the torque on f is not captured in equation (7).

By combining equations (5) and (7), using $K = 2.11$ and $m = 0.223$ (see §2), one finds

$$\frac{\tau_w}{\tau_{\text{dsd}}} \approx 6.0 \times 10^4 \left(\frac{\chi(\beta)}{10^{-2}}\right)^{-1} \left(\frac{f}{0.1}\right)^{-1} \left(\frac{R_*}{r_A}\right)^{2.48}. \quad (8)$$

The lines in figure 1 show equation (8) for $f = 0.1$ and for three different values of β . This includes a line for $\beta = 1$, which corresponds to the strongest possible star-disk spin-down torque (as discussed by MP05b). Even in this case, the fiducial stellar wind torque is ~ 20 times stronger than the star-disk spin-down torque. For smaller, more realistic values of β , the star-disk spin-down torque only becomes weaker, while the stellar wind torque is not affected. It is clear that for the parameters considered here, the angular momentum extracted by the stellar wind completely dominates over that which can be transferred from the star to the disk.

The stellar wind torque becomes weaker relative to

τ_{dsd} when r_A is larger (e.g., for smaller \dot{M}_w) or for more rapidly spinning stars (larger f). For the case of $\beta = 0.01$, favored by MP05b, τ_w will be larger than τ_{dsd} for a star with $f = 0.1$, as long as $r_A \lesssim 84 R_*$. This limiting value is much longer than any of the lever arm lengths listed in table 2. As an example, for all else being equal to the fiducial case, equation (3) suggests that $\tau_w > \tau_{\text{dsd}}$, as long as $\dot{M}_w \gtrsim 3 \times 10^{-14} M_\odot \text{ yr}^{-1}$. This limit is comparable to the solar wind mass loss rate. If the stellar dipole field strength is instead $B_* = 2 \text{ kG}$, the limit becomes $\dot{M}_w \gtrsim 3 \times 10^{-12} M_\odot$.

The squares and triangles in figure 1 represent the data from table 2. Note that nine of the data points (for each β) match the line very well. This is expected since the results from these cases were used to obtain the value of K and m used in equation (8). There are five cases (for each β) that lie slightly off of the line. Three of them represent the last three cases listed in table 2, and the other two are the $f = 0.2$ and $f = 0.05$ cases (which, for the plot, we have scaled by a factor of $f/0.1$, to take into account the spin dependence of equation (8)). These five cases are not expected to match exactly since equation (3) is not precise for cases with different wind driving or spin rates than the fiducial case (see Paper II). Thus, the scatter of these five cases around the line indicates a sort of uncertainty of the semi-analytic formula for the stellar wind, due to variations in the wind driving mechanism and stellar spin rate. It is evident from the figure that this uncertainty does not affect the main conclusion here that stellar wind torques dominate the spin down of the star.

Thus, for the slow rotators ($f \sim 0.1$), we conclude that a stellar wind will transport much more angular momentum from the star than will a magnetic connection to the disk, as long as the stellar wind mass outflow rate is substantially larger than the solar wind mass outflow rate. For the systems considered here, with $\dot{M}_w \sim 10^{-9} M_\odot \text{ yr}^{-1}$, the stellar wind torque completely dominates over any other spin-down torque felt by the star. Since τ_{dsd} is negligible, the only important torques on these stars are the spin-down torque from the stellar wind and the spin-up portion of the star-disk interaction torque. We compare these two torques in the following section.

4. SPIN EQUILIBRIUM BY AN APSW

Section 3 revealed that, for the slow rotators with substantial stellar winds, the spin-down torque felt by the star from the star-disk interaction is negligible. Thus, the spin state of the star is characterized as a competition between the spin-up component of the star-disk interaction torque and the spin-down by the stellar wind. If a system's parameters are measured, the theory can be used to determine the net torque on the star.

Given enough time ($\sim 10^5$ – 10^6 yr for CTTSs), the stellar spin should approach an equilibrium spin state in which the net torque on the star is zero (see, e.g., Cameron & Campbell 1993; Armitage & Clarke 1996). The variability observed in accreting systems (e.g., Hartmann 1997) suggests that spin equilibrium may only represent a time-averaged state, and the condition of net zero torque simply identifies where the net torque changes sign. In any case, it is instructive to examine the conditions of spin-equilibrium.

TABLE 3
SPIN-EQUILIBRIUM RESULTS FOR $\gamma_c = 1$ & $\beta = 0.1$

Case	\dot{M}_w/\dot{M}_a	R_t/R_*	State	ϵ_∞
fiducial	0.43	4.4	2	0.71
$f = 0.2$	0.21	2.9	2	0.39
$f = 0.05$	0.83	5.9	1	1.2
$B_* = 400$ G	0.23	4.5	2	0.37
$B_* = 2$ kG	0.057	4.6	2	0.055
low \dot{M}_w	0.15	4.6	2	0.23
very low \dot{M}_w	0.076	4.6	2	0.094
$R_* = 1.5 R_\odot$	0.58	4.3	2	0.96
$R_* = 3 R_\odot$	0.28	4.5	2	0.46
$M_* = 0.25 M_\odot$	0.37	4.5	2	0.61
$M_* = 1 M_\odot$	0.51	4.4	2	0.84
$c_s/v_{\text{esc}} = 0.245$	0.48	4.4	2	0.87
$c_s/v_{\text{esc}} = 0.192$	0.40	4.4	2	0.61
$\gamma = 1.10$	0.34	4.4	2	0.48

In sections 4.1 – 4.3, we examine the expected spin-equilibrium state of the specific cases of stellar winds simulated in Paper II. In section 4.4, we use the semi-analytic formulation of equation 3 to make more general conclusions.

4.1. Spin Equilibrium for Specific Cases

The spin-up portion of the star-disk interaction torque comes primarily from the accretion of material from the innermost part of the disk onto the star. In this section, we examine some specific cases of spin equilibrium, by determining under what conditions this spin-up torque balances the stellar wind torques for the simulations listed in table 2.

When a star’s magnetic field is strong enough, it will disrupt the Keplerian disk at some radius, R_t , the disk truncation radius. We calculate the location of R_t using the method and equations contained in the Appendix, which follows MP05b. From R_t , accreting material is channeled by the magnetic field to the surface of the star. There is a torque associated with the truncation of the disk and the accretion of material from R_t . This torque, hereafter the “accretion torque,” is given by MP05b as

$$\tau_a = \dot{M}_a \sqrt{GM_* R_*} \left[\left(\frac{R_t}{R_*} \right)^{1/2} - k^2 f \right], \quad (9)$$

where \dot{M}_a is the mass accretion rate onto the stellar surface and k is the normalized radius of gyration of the star (we assume $k^2 \approx 0.2$; Armitage & Clarke 1996). Equation (9) assumes that all of the Keplerian specific angular momentum of the disk material near R_t is transferred to the star. This naturally follows from the dynamical truncation of the disk (e.g., Yi 1995; Wang 1995; MP05b) and is supported by numerical simulations (e.g., Romanova et al. 2002; Long et al. 2005). It is clear that the accretion torque depends both on \dot{M}_a and R_t . At the same time, as shown in the Appendix, the location of R_t itself depends on most of the parameters, including \dot{M}_a and β .

The spin equilibrium state is defined by

$$\tau_a = -\tau_w. \quad (10)$$

Each of our wind simulation cases represents a specific set of values for τ_w , \dot{M}_w , B_* , M_* , R_* , and Ω_* . For each

TABLE 4
SPIN-EQUILIBRIUM RESULTS FOR $\gamma_c = 1$ & $\beta = 0.01$

Case	\dot{M}_w/\dot{M}_a	R_t/R_*	State	ϵ_∞
fiducial	0.44	4.6	2	0.73
$f = 0.2$	0.21	2.9	2	0.39
$f = 0.05$	0.83	5.9	1	1.2
$B_* = 400$ G	0.24	4.6	2	0.39
$B_* = 2$ kG	0.057	4.6	2	0.055
low \dot{M}_w	0.15	4.6	2	0.23
very low \dot{M}_w	0.077	4.6	2	0.096
$R_* = 1.5 R_\odot$	0.59	4.4	1	0.98
$R_* = 3 R_\odot$	0.28	4.6	2	0.46
$M_* = 0.25 M_\odot$	0.38	4.6	2	0.63
$M_* = 1 M_\odot$	0.52	4.6	2	0.86
$c_s/v_{\text{esc}} = 0.245$	0.49	4.6	2	0.88
$c_s/v_{\text{esc}} = 0.192$	0.41	4.6	2	0.62
$\gamma = 1.10$	0.35	4.6	2	0.49

simulation case, we used equation (9) and the method in the Appendix to determine the values of R_t and \dot{M}_a such that the condition (10) is satisfied. We consider both a case with $\beta = 0.1$ and a case with $\beta = 0.01$ (see §3). The results, given as \dot{M}_w/\dot{M}_a and R_t/R_* , are listed in the 2nd and 3rd columns of tables 3 (for $\beta = 0.1$) and 4 (for $\beta = 0.01$).

A comparison between tables 3 and 4 reveals that the disk magnetic coupling parameter β has little influence on the equilibrium values of \dot{M}_a and R_t . This demonstrates that, although β has a large influence on the (negligible) spin-down part of the star-disk interaction torque (as shown in §3), β has very little influence on the spin-up part.

For the specific cases of the simulated stellar winds, it is clear that the equilibrium spin state is characterized by \dot{M}_w/\dot{M}_a of typically a few tens of percent. This ratio is smaller for cases with larger r_A (e.g., for larger field strength or smaller \dot{M}_w). Thus, the cases listed in the tables confirm the general conclusion of Paper I, and represent valid torque solutions for the spin equilibrium state.

4.2. Magnetic Connection State of the System

As pointed out by MP05b (and see the Appendix), an accreting system may exist in a state where the stellar magnetic field connects to the disk outside the corotation radius, which they call “state 2,” and which we implicitly assumed in section 3. On the other hand, if the disk truncation radius is sufficiently smaller than R_{co} , the star can lose its magnetic connection to all but the very inner edge of the disk, which they call “state 1.” The determination of R_t is different in the two states. In the absence of a stellar wind torque, a star in spin equilibrium must be characterized by state 2 (MP05b). Thus, having R_t very close to R_{co} is a requirement of the “disk locking” models (Königl 1991; Ostriker & Shu 1995; Wang 1995). By contrast, this is not a requirement of the APSW scenario.

Following MP05b (using equation A1), we determined the magnetic connection state of the spin-equilibrium systems described above and listed this in the 4th column of tables 3 and 4. Note that MP05b only consider a loss of magnetic connection via the differential twisting of field lines. The stellar wind should also influence the

connectedness between the star and disk (Safier 1998), but we do not attempt to quantify this here.

Tables 3 and 4 reveal that most (though not all) of the simulated cases are in a magnetic connection state 2, while in spin-equilibrium. A characteristic of this state is that R_t is very close to R_{co} , which is also evident in the tables ($R_{co}/R_* = 7.4, 4.6$, and 2.9 for $f = 0.05, 0.1$, and 0.2 , respectively). It appears that, when a stellar wind torque balances the accretion torque, it may be common (though not required) for the disc truncation radius to be close to the corotation radius (unless the spin rate is substantially less than $f = 0.1$).

4.3. Accretion Power

In the APSW scenario proposed in Paper I, the energy that powers the stellar wind ultimately comes from the energy released by the accretion process. In this section, we calculate what fraction of the accretion power would be required to drive the wind, in the specific cases for which we have determined the spin-equilibrium.

In order to tabulate the accretion power, the precise details of the complicated interaction between the star and disk are not important. The general behavior is that material from the Keplerian disk becomes attached to the stellar magnetosphere near R_t and eventually falls onto and becomes part of the star. Energetically, this can be treated as an inelastic process, wherein only the energy content before and after the interaction needs to be specified. Thus, the rate of potential energy release is simply $1/2 \dot{M}_a v_{esc}^2 (1 - R_*/R_t)$. Note that as accreting material piles onto the stellar surface, there should be additional energy released as material either “sinks” into (convectively) or compresses the star. This is another potential energy source, but we neglect this here. The rate of (rotational) kinetic energy release is $1/4 \dot{M}_a v_{esc}^2 (R_*/R_t - k^2 f^2)$, where the last term assumes that accreting material eventually achieves the same specific angular momentum as the star. The difference in thermal energy density between material at the disk inner edge and material at stellar photospheric temperature is negligible compared to the potential and kinetic energy release. Thus, by summing the potential and kinetic energies, the rate of energy release in the vicinity of the star is approximately

$$\dot{E}_a = \frac{1}{2} \dot{M}_a v_{esc}^2 \left(1 - \frac{1}{2} \frac{R_*}{R_t} - \frac{1}{2} k^2 f^2 \right). \quad (11)$$

Since there is an accretion torque on the star, some of this energy is added to the rotational energy of the star at a rate $\Omega_* \tau_a$. The remaining energy ($\dot{E}_a - \Omega_* \tau_a$) is available to power other accretion-related activity³. In particular, this remaining energy is responsible for powering the observed excess continuum emission (such as the UV excess) and line emission (e.g., Königl 1991; Calvet & Gullbring 1998; Muzerolle et al. 2001), in addition to driving an enhanced stellar wind (Paper I).

Paper I proposed that a fraction ϵ of this energy specifically powers the thermal energy in the stellar wind. Our

³ We follow a similar derivation of the accretion power to that of Paper I, where equation (4) of that work corresponds to the remaining energy, $\dot{E}_a - \Omega_* \tau_a$, and neglects terms proportional to f^2 .

simulated winds are thermally driven, but the wind driving mechanism at work in real systems is still uncertain (see Paper II). Thus, we wish to calculate the power required to drive the wind, in a generic form. For this, we simply calculate the total energy in the wind far from the star plus the potential energy required to lift the wind off the stellar surface. In this way, the power in a steady-state, 2.5D, MHD wind can be obtained by (see, e.g., Ustyugova et al. 1999; Keppens & Goedbloed 2000)

$$\dot{E}_w = 4\pi R^2 \int_0^1 \rho v_R E' d(\cos \theta) + \frac{1}{2} \dot{M}_w v_{esc}^2, \quad (12)$$

where θ is the usual spherical coordinate and

$$E' \equiv \frac{v_p^2 + v_\phi^2}{2} + \frac{B_\phi^2}{4\pi\rho} - \frac{v_\phi B_\phi B_p}{4\pi\rho v_p}. \quad (13)$$

In equation (13), we have neglected the thermal and gravitational potential energy, so the integral in equation (12) should be evaluated at large R , where E' has reached an asymptotic value and these energies are negligible. Thus, \dot{E}_w represents the total power required to lift material off of the star, to accelerate it to the wind velocity, and to provide the magnetic energy content carried with the wind.

For each of our simulated wind solutions, we evaluate the integral in equation (12) at a radius of $R = 50R_*$, where E' is within a few percent of its asymptotic value. The spin of the star does work on the wind at a rate $\Omega_* \tau_w$. This represents the power injected in the wind by magnetocentrifugal processes. We find that the ratio $\Omega_* \tau_w / \dot{E}_w$ is 30% in the fiducial case. In most other cases, the value of this ratio falls the range 10–60%. This indicates that, as discussed by Paper I and II (and see Washimi & Shibata 1993), these winds are in a regime where the magnetocentrifugal effects are of nearly equal importance with the other source of wind driving.

It is this other source of wind driving that we propose is powered by some fraction of the available accretion energy. We define this fraction as⁴

$$\epsilon_\infty \equiv \frac{\dot{E}_w - \Omega_* \tau_w}{\dot{E}_a - \Omega_* \tau_a}. \quad (14)$$

This represents the minimum fraction of the accretion power required to drive the stellar wind, since whatever mechanism drives the wind will not itself likely be 100% efficient (Decampli 1981).

In the last column of tables 3 and 4, we list the value of ϵ_∞ for each case in spin-equilibrium. In one case ($f = 0.05$), ϵ_∞ is greater than 100%, indicating that there is not enough accretion power in the spin equilibrium state to power the wind. This case is therefore not an acceptable solution for a system in spin-equilibrium by an APSW. All of the other cases have $\epsilon_\infty < 1$, and so they are energetically viable solutions.

There is a relationship between ϵ_∞ , the observed excess emission, and the inferred mass accretion rate. In

⁴ This fraction is a more general definition than ϵ in Paper I, which assumes thermal wind driving. By contrast, ϵ_∞ is the fraction of the accretion power required to explain the energy in the wind at large distances from the star, regardless of the driving mechanism.

particular, the accretion rates are typically determined by measuring excess emission and assuming that all of the accretion power is radiated (e.g., Calvet & Gullbring 1998). In the APSW scenario, some of the accretion power drives the stellar wind, so only a fraction $1 - \epsilon_\infty$ of the accretion power can be radiated. This means that the true accretion rate (\dot{M}_a) will be a factor of $(1 - \epsilon_\infty)^{-1}$ larger than the observationally determined value. In this context, and since ϵ_∞ is the minimum required fraction to drive the wind, a value of $\epsilon_\infty \gtrsim 0.5$ (as for several cases listed in tables 3 and 4) appears quite large. However, the observational determination of \dot{M}_a is uncertain by a factor of several, as exemplified by the large range of measurements compiled by Johns-Krull & Gafford (2002). Thus, while it is clear that $\epsilon_\infty < 1$ is a hard upper limit, it is not yet clear how close to unity ϵ_∞ can be.

As expected, the cases with lower values of \dot{M}_w/\dot{M}_a (i.e., cases with larger field strength or smaller \dot{M}_w) require a smaller fraction of the accretion power to drive the wind. The cases in the table suggest approximately that $\epsilon_\infty \approx 1.6\dot{M}_w/\dot{M}_a$. Thus, it appears that $\dot{M}_w/\dot{M}_a \lesssim 0.6$ represents a hard upper limit for APSWs.

It is important to note that the manner in which the accretion power transfers to the stellar wind is still unspecified in the APSW model. This will depend upon what is the wind driving mechanism, which is currently unknown. In reality, the physics of the energy coupling will likely determine the value of ϵ_∞ , which effectively sets the value for \dot{M}_w/\dot{M}_a . Then, given enough time, the stellar spin rate will evolve toward the equilibrium value set primarily by \dot{M}_w/\dot{M}_a and r_A/R_* . Thus the spin-equilibrium state of the star is ultimately determined by the power coupling and magnetic properties, and more work is needed to take this further.

4.4. Semi-Analytic Formulation for Spin Equilibrium

In order to develop a more general, predictive theory, in this section we make use of the semi-analytic formulation of equation (3). As justified by the previous sections, we assume that the equilibrium spin rate of the star is simply determined by a balance between the spin-up torque from accretion and the spin-down torque from the stellar wind. Using equations (1) – (3), (9), and (10), we can write the stellar wind equilibrium spin rate, expressed as a fraction of breakup spin, as

$$f_{sw} = K^{-2} \left(\frac{R_t}{R_*} \right)^{1/2} \left(\frac{\dot{M}_a}{\dot{M}_w} \right)^{1-2m} \Psi^{-2m}, \quad (15)$$

where

$$\Psi \equiv \frac{B_*^2 R_*^2}{\dot{M}_a v_{esc}} \quad (16)$$

is a dimensionless magnetization parameter⁵. Here, we have neglected the term proportional to $k^2 f$ in equation (9), since it is generally much smaller than the other term. Again, note that a weak f -dependence of r_A is not included in equation (3), so the dependence of f_{sw}

on some of the parameters is not precisely captured in equation (15) (see Paper II).

Equation (15) includes a dependence on the truncation radius of the disk, R_t . This location itself has a dependence on the other parameters, and the determination of R_t depends on the magnetic connection state of the system (§4.2; MP05b). In general, R_t depends on Ψ , but if R_t is close to the corotation radius, R_{co} , then R_t also depends on the stellar spin rate. We will consider two cases that are expected to bracket reality.

The first case is one in which the system is in state 1 as defined by MP05b. Here, R_t does not depend on the stellar spin rate, and it is simply proportional to the original calculations by Lamb et al. (1973) and Davidson & Ostriker (1973) used in most Ghosh & Lamb type models. Thus, using equation (A2) for R_t , adopting $\gamma_c = 1$, and plugging in to equation (15), one finds

$$f_{sw1} = \frac{2^{3/14}}{K^2} \left(\frac{\dot{M}_a}{\dot{M}_w} \right)^{1-2m} \Psi^{1/7-2m}. \quad (17)$$

This is the predicted equilibrium spin rate when the truncation radius is significantly smaller than the corotation radius (i.e., in magnetic connection state 1).

The second case to consider is where $R_t \approx R_{co}$, which is the requirement of all disk-locking models (Shu et al. 1994; Wang 1995, MP05b). Using equation (4) and setting $R_t = R_{co}$ in equation (15), one finds

$$f_{sw2} = K^{-3/2} \left(\frac{\dot{M}_a}{\dot{M}_w} \right)^{(3-6m)/4} \Psi^{-3m/2}. \quad (18)$$

This is the predicted equilibrium spin rate when the disk truncation occurs very close to R_{co} .

Which case is more appropriate? The first case is expected to occur for relatively small values of Ψ and low spin rates f (MP05b), and the opposite is true for the second case. For the parameter space we have considered thus far in this work, we found in section 4.2 that most (though not all) of the cases are expected to have R_t/R_{co} near unity. Thus, while it is not a formal requirement of APSW, it may often be the case that $R_t \approx R_{co}$ for systems in spin equilibrium, and we will focus on this second case for the remainder of this work.

Figure 2 shows the predicted spin rate of this case (eq. 18) versus Ψ , for many different values of the ratio \dot{M}_w/\dot{M}_a . The results of section 4.3 indicate that the accretion power is only capable of powering a wind with $\dot{M}_w/\dot{M}_a \lesssim 0.6$, and this is a hard upper limit. This “forbidden” region of the f - Ψ space is indicated in figure 2.

The plot also shows the simulation results (squares). The value of Ψ for each case is determined mostly by input parameters but also by \dot{M}_a . The latter was set (in section 4.1) by the condition that the equilibrium spin rate was equal to the value of f used as the simulation input parameter. The squares indicate the range over which equation (18) is shown to be valid by the simulations. Also, the plot shows the specific case of $K = 2.11$ and $m = 0.223$.

The results shown in figure 2 and equation (18) provide the basis for predictions of the APSW model that can be observationally tested and constrained, and that can be

⁵ The magnetization parameter Ψ is related to ψ used by MP05b (see their eq. 16) by a constant factor, $\psi = 2^{3/2}\Psi$.

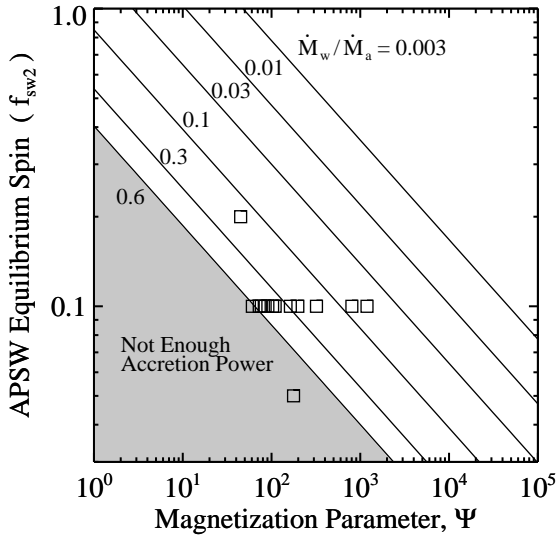


FIG. 2.— The equilibrium spin rate predicted by a balance between the spin down from a stellar wind and the spin up from accretion, versus the dimensionless magnetization parameter $\Psi \equiv B_*^2 R_*^2 (\dot{M}_a v_{\text{esc}})^{-1}$. The solid lines show equation (18) for $K = 2.11$, $m = 0.223$ and several different possible values of \dot{M}_w/\dot{M}_a , as indicated. The squares show data from table 3, which indicates the range of parameters considered in our simulations and used to derive equation (18). The shaded region corresponds approximately to where accretion power is not sufficient to drive the stellar wind.

compared to other models. Different theories predict different power laws for f vs. Ψ . Specifically, equation (18) predicts a power law index of ≈ -0.33 , the conditions appropriate for equation (17) predict ≈ -0.30 , and an index of $-3/7$ is predicted by the disk locking models (e.g., Königl 1991; Shu et al. 1994).

5. SUMMARY AND DISCUSSION

In this work, we have further developed the accretion-powered stellar wind model proposed in Paper I, where the stellar wind magnetic lever arm length, r_A , was taken as a parameter to determine the stellar wind torque. We employed the simulation results of Paper II (see §2) to obtain stellar wind torques for several cases representative of T Tauri systems. We examined the total torque on the star arising from the stellar wind plus the magnetic interaction between the star and its accretion disk. Our results can be summarized as follows.

1. We found that the spin-down torque from a stellar wind can be orders of magnitude stronger than the spin-down portion of the star-disk interaction torque, for slowly rotating stars with mass loss rates substantially larger than the solar wind outflow rate (see §3). This confirms the assumption of Paper I that the condition for net zero torque on the star (spin equilibrium) is simply determined by a balance between the stellar wind torque and the accretion torque.
2. Using the computed stellar wind torques for several cases, we looked at the conditions for spin equilibrium (§4.1). We found that a rotation rate of 10% of breakup speed typically requires \dot{M}_w/\dot{M}_a equal

a few tens of percent, confirming the original suggestion by Hartmann & Stauffer (1989) that stellar winds may be capable of removing accreted angular momentum.

3. For most cases in spin equilibrium, the disk truncation radius was very close to the corotation radius, though this is not a general requirement of the APSW model (§4.2).
4. Accretion power is generally sufficient to power a stellar wind that is capable of solving the angular momentum problem (§4.3), as suggested in Paper I. The energy requirements for most of the cases considered here is relatively large, and more work is needed to further constrain the energy coupling.
5. Under the assumption that the stellar wind is accretion powered, the cases we examined suggested a hard upper limit of $\dot{M}_w/\dot{M}_a \lesssim 0.6$.
6. Finally, in section 4.4 we used the results from Paper II to derive a semi-analytic formulation for the equilibrium spin rate predicted by the APSW model. We found that the spin rate, expressed as a fraction of breakup speed, generally depends only on the two dimensionless parameters \dot{M}_w/\dot{M}_a and $\Psi \equiv B_*^2 R_*^2 (\dot{M}_a v_{\text{esc}})^{-1}$.

The APSW model incorporates several previous ideas. As in all other models that emphasize the role of stellar magnetic fields, the interaction of the magnetized star with the disk leads to the truncation of the disk and accretion of material along field lines onto the star. The APSW model adopts the finding of the Ghosh & Lamb-type models (e.g., Ghosh & Lamb 1978; Königl 1991; Armitage & Clarke 1996), which is also supported by numerical simulations (Romanova et al. 2002; Long et al. 2005), that the angular momentum of accreting material is transferred to the star. However, in contrast to the Ghosh & Lamb-type models, we found that for slow rotators, any spin-down torque arising from the star-disk interaction is negligible (item 1 above). Instead, the stellar spin-up torque from accretion is counteracted by an accretion-driven stellar wind, which carries a comparable amount of angular momentum out of the system.

Compared to all existing models, APSW is distinct in that it conceptually links the driving of the stellar wind to the energy released by the accretion process (via ϵ). In other words, the general picture of APSW is similar to other angular momentum models that utilize winds. In particular, the X-wind (Shu et al. 1994; Ostriker & Shu 1995), the Reconnection X-wind (Ferreira et al. 2000), and other works considering stellar winds (Hartmann & Stauffer 1989; Paatz & Camenzind 1996) all find that, in order to carry away significant angular momentum, the mass outflow rate needs to be of the order of 10% of the accretion rate (item 2 above). Except for the X-wind, in all of the above scenarios, the outflow is magnetically connected to the star, and thus extracts angular momentum directly from the star. By contrast, the X-wind outflow is magnetically connected to the disk. Furthermore, the X-wind is unique in that it assumes that the accretion of material does not deposit angular momentum onto the star.

As mentioned in item 3 above, for most of the specific cases of our simulated winds, we found that in the spin equilibrium state, the truncation radius was very close to the corotation radius. This is similar to the prediction of the disk locking models, which includes both the Ghosh & Lamb-type models and the X-wind. However, in contrast with the disk locking models, it is not a requirement of APSW that R_t be close to R_{co} . Measurements of the location of the inner edge of the gas disk (Najita et al. 2003; Carr 2007) suggest that R_t/R_{co} is typically $\sim 70\%$. We leave a more detailed comparison between models for future work.

There is observational evidence that the outflow rates from accreting young stellar systems are of the order of 10% of the accretion rates (e.g., Hartigan et al. 1995; Calvet 1997) and are therefore accretion powered (Cabrit et al. 1990). However, it appears that a large fraction of this flow (which is usually probed by forbidden emission coming from large spatial scales) originates in the disk, rather than the star (Ferreira et al. 2006). It is not yet clear how much of the total observed flow may originate in a stellar wind. There is some evidence specifically for stellar winds from CTTSs (Beristain et al. 2001; Edwards et al. 2003; Dupree et al. 2005; Edwards et al. 2006; Kwan et al. 2007), as distinct from disk winds, and that these are accretion powered (e.g., Edwards et al. 2003, 2006), but the mass outflow rates are not yet well constrained (Dupree et al. 2005). Additional work constraining the value of \dot{M}_w/\dot{M}_a , the stellar wind driving mechanism, and the stellar magnetic field strength and geometry will help to provide stringent and quantitative tests for the APSW model.

The predictions of the spin equilibrium state can also be checked observationally (Johns-Krull & Gafford 2002). This will likely require large samples of stars, due to large uncertainties in measured parameters, and since intrinsic variability in real systems (Hartmann 1997, e.g.) may only allow a spin equilibrium state to be achieved in a time-averaged sense. The Ghosh & Lamb, X-wind, and APSW models all predict an equilibrium spin rate that depends on Ψ , but of these three, only the

APSW model contains an additional dependence on the stellar wind mass outflow rate. For the power law fits to the simulations of Paper II, the APSW spin equilibrium predicts a slightly different power-law of spin vs. Ψ than the other models (§4.4)—though the exact dependence of the stellar wind torque has not been determined for all parameters.

In this series of papers, we have focused on the global problem of calculating the magnitude of stellar wind torques and comparing them with other torques acting on accreting stars. In order to refine the APSW model further and make the predictions more precise, more work is required. In particular, it is not yet clear how the presence of an accretion disk will influence the stellar wind torque, and conversely, how a stellar wind may influence the accretion process. Also, although it is clear that there is enough accretion energy to power the stellar wind, it is still not known what actually drives the stellar wind and how the accretion power may transfer to it. We suspect that a strong flux of hydromagnetic waves can be excited near the base of the accretion shock and can tap the energy released there, which may provide an efficient driver for the APSW. We defer a rigorous investigation of the APSW driving mechanism to future work.

We wish to thank many people for discussions regarding this work, including: Gibor Basri, Sylvie Cabrit, Andrea Dupree, Suzan Edwards, Will Fischer, Shu-ichiro Inutsuka, Chris Johns-Krull, Marina Romanova, Frank Shu, Keivan Stassun, Jeff Valenti, and Sydney Wolff. We also thank the referee, Jonathan Ferreira, for his useful suggestions for improving the paper and KITP for hosting us while finishing the manuscript. This research was supported in part by the National Science Foundation under Grant No. PHY05-51164. SM is supported by the University of Virginia through a Levinson/VITA Fellowship partially funded by The Frank Levinson Family Foundation through the Peninsula Community Foundation. REP is supported by a grant from NSERC.

APPENDIX

DETERMINATION OF THE DISK TRUNCATION RADIUS

We follow MP05b to calculate the location of the disk truncation radius, R_t , and the reader will find details in that paper. For convenience, we list the relevant equations here. As in section 3, we adopt $\gamma_c = 1$.

To determine R_t , we first find the magnetic connectivity state using the criterion

$$f < (1 - \beta)(2^{3/2}\Psi)^{-3/7}, \quad (A1)$$

where Ψ is defined by equation (16). If condition (A1) is satisfied, the system is in “state 1.” Otherwise, it is in “state 2.” In state 1, we determine the truncation radius using

$$R_t = (2^{3/2}\Psi)^{2/7} R_*. \quad (A2)$$

In state 2, we determine the truncation radius by solving

$$\left(\frac{R_t}{R_{co}}\right)^{-7/2} \left[1 - \left(\frac{R_t}{R_{co}}\right)^{3/2}\right] = \frac{\beta}{2^{3/2}\Psi} f^{-7/3}. \quad (A3)$$

REFERENCES

- Armitage, P. J. & Clarke, C. J. 1996, MNRAS, 280, 458
 Beristain, G., Edwards, S., & Kwan, J. 2001, ApJ, 551, 1037
 Bertout, C., Basri, G., & Bouvier, J. 1988, ApJ, 330, 350
 Bouvier, J., Forestini, M., & Allain, S. 1997, A&A, 326, 1023

- Cabrit, S., Edwards, S., Strom, S. E., & Strom, K. M. 1990, *ApJ*, 354, 687
- Calvet, N. 1997, in *IAU Symposium*, Vol. 182, *Herbig-Haro Flows and the Birth of Stars*, ed. B. Reipurth & C. Bertout, 417–432
- Calvet, N. & Gullbring, E. 1998, *ApJ*, 509, 802
- Camenzind, M. 1990, in *Reviews in Modern Astronomy*, ed. G. Klare, 234–265
- Cameron, A. C. & Campbell, C. G. 1993, *A&A*, 274, 309
- Carr, J. S. 2007, to appear in proceedings of IAU Symposium No. 243, *Star-Disk Interaction in Young Stars*
- Davidson, K. & Ostriker, J. P. 1973, *ApJ*, 179, 585
- Decamp, W. M. 1981, *ApJ*, 244, 124
- Dupree, A. K., Brickhouse, N. S., Smith, G. H., & Strader, J. 2005, *ApJ*, 625, L131
- Edwards, S., Fischer, W., Hillenbrand, L., & Kwan, J. 2006, *ApJ*, 646, 319
- Edwards, S., Fischer, W., Kwan, J., Hillenbrand, L., & Dupree, A. K. 2003, *ApJ*, 599, L41
- Ferreira, J. 1997, *A&A*, 319, 340
- Ferreira, J., Dougados, C., & Cabrit, S. 2006, *A&A*, 453, 785
- Ferreira, J., Pelletier, G., & Appl, S. 2000, *MNRAS*, 312, 387
- Ghosh, P. & Lamb, F. K. 1978, *ApJ*, 223, L83
- Hartigan, P., Edwards, S., & Ghandour, L. 1995, *ApJ*, 452, 736
- Hartmann, L. 1997, in *IAU Symposium*, Vol. 182, *Herbig-Haro Flows and the Birth of Stars*, ed. B. Reipurth & C. Bertout, 391–405
- Hartmann, L. & Stauffer, J. R. 1989, *AJ*, 97, 873
- Herbst, W., Eislöffel, J., Mundt, R., & Scholz, A. 2007, in *Protostars and Planets V*, ed. B. Reipurth, D. Jewitt, & K. Keil, 297–311
- Jayawardhana, R., Coffey, J., Scholz, A., Brandeker, A., & van Kerkwijk, M. H. 2006, *ApJ*, 648, 1206
- Johns-Krull, C. M. & Gafford, A. D. 2002, *ApJ*, 573, 685
- Joy, A. H. 1945, *ApJ*, 102, 168
- Keppens, R. & Goedbloed, J. P. 2000, *ApJ*, 530, 1036
- Königl, A. 1991, *ApJ*, 370, L39
- Kwan, J., Edwards, S., & Fischer, W. 2007, *ApJ*, 657, 897
- Lamb, F. K., Pethick, C. J., & Pines, D. 1973, *ApJ*, 184, 271
- Long, M., Romanova, M. M., & Lovelace, R. V. E. 2005, *ApJ*, 634, 1214
- Lynden-Bell, D. & Pringle, J. E. 1974, *MNRAS*, 168, 603
- Lyo, A.-R. & Lawson, W. A. 2005, *Journal of Korean Astronomical Society*, 38, 241
- Matt, S. & Pudritz, R. E. 2005a, *ApJ*, 632, L135 (Paper I)
- . 2005b, *MNRAS*, 356, 167 (MP05b)
- . 2007, to appear in proceedings of the 14th Cambridge Workshop on Cool Stars, Stellar Systems, and the Sun, astro-ph/0701648
- . 2008, *ApJ*, in press (arXiv:0801.0436) (Paper II)
- Muzerolle, J., Calvet, N., & Hartmann, L. 2001, *ApJ*, 550, 944
- Najita, J., Carr, J. S., & Mathieu, R. D. 2003, *ApJ*, 589, 931
- Ostriker, E. C. & Shu, F. H. 1995, *ApJ*, 447, 813
- Paatz, G. & Camenzind, M. 1996, *A&A*, 308, 77
- Pelletier, G. & Pudritz, R. E. 1992, *ApJ*, 394, 117
- Rebull, L. M., Wolff, S. C., & Strom, S. E. 2004, *AJ*, 127, 1029
- Rebull, L. M., Wolff, S. C., Strom, S. E., & Makidon, R. B. 2002, *AJ*, 124, 546
- Romanova, M. M., Ustyugova, G. V., Koldoba, A. V., & Lovelace, R. V. E. 2002, *ApJ*, 578, 420
- Safer, P. N. 1998, *ApJ*, 494, 336
- Shakura, N. I. & Sunyaev, R. A. 1973, *A&A*, 24, 337
- Shu, F., Najita, J., Ostriker, E., Wilkin, F., Ruden, S., & Lizano, S. 1994, *ApJ*, 429, 781
- Tout, C. A. & Pringle, J. E. 1992, *MNRAS*, 256, 269
- Ustyugova, G. V., Koldoba, A. V., Romanova, M. M., Chechetkin, V. M., & Lovelace, R. V. E. 1999, *ApJ*, 516, 221
- Uzdensky, D. A. 2004, *Ap&SS*, 292, 573
- Uzdensky, D. A., Königl, A., & Litwin, C. 2002, *ApJ*, 565, 1191
- Vogel, S. N. & Kuhi, L. V. 1981, *ApJ*, 245, 960
- Wang, Y.-M. 1995, *ApJ*, 449, L153
- Washimi, H. & Shibata, S. 1993, *MNRAS*, 262, 936
- Yi, I. 1995, *ApJ*, 442, 768